

The Development of Metal-Carbon Catalysts for Oxidative Desulfurization of Diesel Fractions

Z.R. Ismagilov, E.V. Matus*, O.S. Efimova, L.M. Khitsova, A.N. Popova, A.P. Nikitin, S.A. Sozinov

Federal Research Center of Coal and Coal Chemistry SB RAS, 18, Sovetsky ave., Kemerovo, Russia

Article info

Received:
16 November 2019

Received in revised form:
28 January 2020

Accepted:
10 March 2010

Keywords:

Carbon nanomaterials
Metal nanoparticles
Catalyst
Oxidative desulfurization

Abstract

Metal-carbon materials M/CNTs (M = Ce, Cu, Mo) were synthesized by incipient wetness impregnation and their physicochemical characteristics were studied using various methods (inductively coupled plasma optical emission spectrometry, thermal analysis coupled with mass spectrometry, low-temperature nitrogen adsorption, X-ray diffraction and structural analysis, scanning electron microscopy, and Raman spectroscopy). It was found that M/CNTs (M = Ce, Cu, Mo) are the mesoporous materials consisting of carbon nanotubes with deposited CeO₂, Cu₂O/Cu or MoO₃/MoO₂ particles, respectively. The dispersion of supported species and their deposition uniformity improve in the series Cu < Ce < Mo. The type of metal was shown to affect thermal stability as well as the textural and structural properties of the samples. The thermal stability of materials increases in the series Ce < Cu ≈ Mo, which is caused by different redox properties of the metals and also by the composition of products of the metal precursor decomposition. It is promising to use the developed materials as the catalysts for deep purification of diesel fraction components from sulfur compounds.

1. Introduction

The necessity to provide ecologically safe and sustainable development of society at a growing consumption of energy resources implies a decrease in discharge of harmful wastes to the environment. However, technogenic emission of SO₂ to the atmosphere still remains high, reaching 3.7 million tons a year in Russia [1]. Contamination of the atmosphere by sulfur dioxide raises the acidity of rain, thus deteriorating natural reforestation, and leads to corrosion of steel constructions and development of bronchopulmonary diseases. Contamination of the atmosphere with sulfur oxides is caused mostly by fuel combustion. Sulfur compounds are present in all commercial fuels, and restrictions on their content become more and more severe. In particular, for diesel fuel corresponding to the requirements of Euro-3, Euro-4 and Euro-5, the sulfur content should not exceed 350, 50 and 10 mg/kg, respectively [2]. In this connection, the development of technologies for reducing the

concentration of sulfur compounds in hydrocarbon feedstock is an urgent problem.

At present, the main industrial method for desulfurization of components of diesel fractions is their catalytic hydrodesulfurization [3, 4]. Economical advisability of this method decreases with stiffening of environmental requirements to the fuel quality, which makes it necessary to develop new approaches to the purification of hydrocarbon feedstock. Oxidative desulfurization (ODS) is among promising alternative methods for the removal of sulfur compounds and has considerable advantages over hydrodesulfurization [5–15]. The ODS process can be performed at lower temperatures and pressures and does not require the use of hydrogen, which is an expensive reagent. Such inexpensive reagents as air oxygen, hydrogen peroxide or organic peroxides can be used as the oxidants.

The ODS catalysts are represented by a wide range of systems including various combinations of catalyst and oxidant: Mo-Al₂O₃/tert-butyl peroxide [16], Mo-SiO₂/H₂O₂ [17], AC/H₂O₂ [18], Pd-MWCNT/H₂O₂ [19], Cr₂O₃-Al₂O₃/H₂O₂ [20],

*Corresponding author. E-mail: matus@catalysis.ru

V₂O₅-TiO₂/H₂O₂ [21], Mo-V-W-P heteropolyacids/O₂ [22], MnO₂-Al₂O₃/O₂ and Co₃O₄-Al₂O₃/O₂ [23]. Catalysts containing complexes of transition metals (Nb, Mo) with crown ethers [24] are also being devised. Transition metal catalysts have a high content of the active component (16 wt.% Mo – 4 wt.% W [16], 12 wt.% Mo [17]), whereas the content of noble metals does not exceed 1 wt.% (0.1 wt.% Pd [19], 0.015 wt.% Au [25], 1 wt.% Pd [20]). A combination of high adsorption capacity to the substrate and ability to activate the oxidant is a necessary condition for creating the catalytic systems efficient in ODS. It was shown [19] that carbon nanomaterials (CNMs) can serve as the promising materials for ODS. The oxidation of sulfur-containing compounds was studied in the presence of carbon nanotubes (CNTs) [26], reduced graphene oxide (rGO) [27], and Au/CNT composites [25].

In order to develop the efficient catalysts for ODS of motor fuels, metal-carbon materials M/CNTs (M = Ce, Cu, Mo) were synthesized in this work, and their properties were investigated using various physicochemical methods.

2. Experimental

Metal-carbon materials M/CNTs (M = Ce, Cu, Mo) were synthesized by incipient wetness impregnation. To this end, Taunit carbon nanotubes (NanoTechCenter Ltd., Tambov, Russia) [28, 29] were impregnated with an aqueous solution of the corresponding metal salt (Ce(NO₃)₃·6H₂O, CuSO₄·5H₂O, (NH₄)₆Mo₇O₂₄·4H₂O) with a specified concentration. After that, the samples were dried in a drying oven in an air medium at 80 °C during 6 h and then calcined in a flow reactor in an argon flow at 600 °C for 2 h.

The elemental composition of the samples was determined by inductively coupled plasma optical emission spectrometry on an atomic emission spectrometer iCAP 6500 Duo LA (ThermoFisher-Scientific, USA).

Thermal analysis (differential thermal analysis (DTA), thermogravimetric analysis (TGA) and differential thermogravimetric analysis (DTG)) of the samples was carried out on an STA 449 F3 Jupiter® (NETZSCH Gerätebau GmbH, Germany) thermoanalyzer over the temperature range of 25–1000 °C at a heating rate 5 °C/min in an N₂ atmosphere.

Textural characteristics of the materials (specific surface area S_{BET}, pore volume V_{pore} and average

pore diameter D_{pore}) were examined on an automated volumetric setup ASAP 2400 (Micromeritics, USA) by measuring and processing the low-temperature nitrogen adsorption isotherms taken at 77 K.

X-ray diffraction and structural analysis (XRD and XSA) of the samples was carried out on a powder X-ray diffractometer Bruker D8 ADVANCE A25 (Bruker, Germany) (CuKα radiation, λ = 1.5406 Å, Ni filter with secondary radiation) at room temperature using polycrystal method. XRD analysis was made using the diffraction patterns obtained by scanning over the angular region 2θ = 10° – 90° with a step 0.02° and accumulation time 2 s. Diffraction peaks were identified by means of ICDD and PDF2 powder diffraction databases. Sizes of the coherent scattering regions (CSR) were calculated using the Debye – Scherrer formula:

$$D_{hkl} = \frac{0.9\lambda}{\beta_{hkl} \cos\theta_{hkl}}$$

where *h*, *k*, *l* are the Miller indices; *D_{hkl}* – the CSR size along the direction perpendicular to (*hkl*) planes; λ – the X-ray wavelength (λ = 1.5406 Å); β_{*hkl*} – the true physical broadening of the line of the tested sample; cosθ_{*hkl*} – the cosine of the X-ray diffraction angle.

Raman spectra were recorded in the spectral shift range of 100–4000 cm⁻¹ on a Raman spectrometer Renishaw Invia (Renishaw plc., UK) with excitation by an argon laser with the wavelength 514.5 nm, diffraction lattice 1800 l/mm and L50× objective. Laser power on a sample did not exceed 0.175 mW, and the accumulation time of useful signal was 120 s.

Scanning electron microscopy (SEM) images were recorded on a JEOL JSM-6390 LA (JEOL, Japan) electron microscope with an X-ray energy dispersive detector JED 2300.

3. Result and discussion

Table lists the parameters of thermal genesis and the main physicochemical properties of the synthesized M/CNT (M = Ce, Cu, Mo) samples.

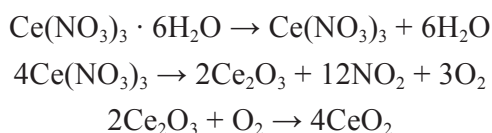
Thermal analysis revealed [30] that heating of the dried samples in an inert atmosphere leads to decomposition of salts – precursors of metals and to a partial degradation of the carbon matrix. The temperature at which M/CNT starts to degrade (T_d) depends on the nature of a metal precursor compound and increases in the series Ce < Cu ≈ Mo (see Table). Different thermal stability of M/CNTs

Table
Parameters of thermal genesis and basic physicochemical properties of M/CNT (M = Ce, Cu, Mo)

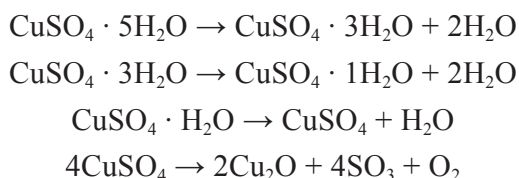
Sample	T _d , °C	M Content, %, mass	Textural characteristics			XRD data			Raman spectroscopy data, I _D /I _G
			S _{BET} , m ² /g	V _Σ , cm ³ /g	D pores, nm	Phase composition	a*, Å	CSR**, nm	
CNT	500	–	180	0.33	7.5	MgO-NiO Ni	4.195 3.529	19 28	1.93
Ce/CNT	230	4.7±0.2	158	0.29	7.4	MgO-NiO Ni CeO ₂	4.195 3.530 5.413	28 37 8	1.81
Cu/CNT	300	4.1±0.1	151	0.30	7.9	MgO-NiO Ni Cu ₂ O Cu	4.187 3.533 4.279 3.620	24 32 20 40	1.96
Mo/CNT	300	4.3±0.1	129	0.28	8.6	MgO-NiO Ni MoO ₂ MoO ₃	4.198 3.524 - -	24 32 - -	1.78

* – cell parameter; ** – coherent scattering region

may be caused by features of the interaction between precursor compound and functional groups of CNTs as well as by the composition of the gas medium formed upon decomposition of inorganic salt. In particular, the decomposition of cerium nitrate hexahydrate is accompanied by the formation of nitrogen oxide and oxygen [31], which serve as oxidants of the carbon matrix:

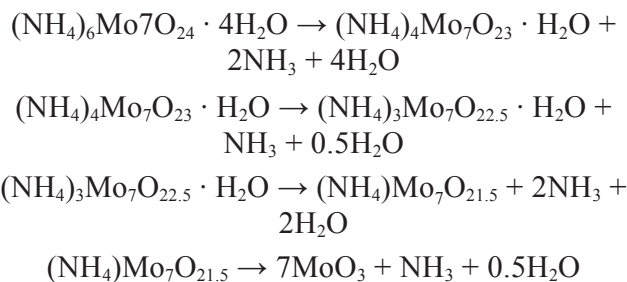


The decomposition of copper sulfate is a multistep process leading to a release of SO₂ and O₂ [32, 33]:



In addition, the reduction of copper cations (Cu²⁺ → Cu⁺ → Cu⁰) in the presence of a carbon matrix cannot be ruled out.

The decomposition of ammonium paramolybdate tetrahydrate is accompanied by the formation of some intermediate compounds and a release of ammonia to the gas medium [34, 35]:



According to the low-temperature nitrogen adsorption, the adsorption isotherms of type IV with the hysteresis loop of H3 type at p/p₀ above 0.45 are observed for M/CNTs, which testify to the presence of mesopores. The specific surface area of the samples is lower as compared to the initial support (see Table). This may be caused by the blocking of thin pores by the active component particles. This effect becomes more pronounced in the series Ce < Cu < Mo. The pore volume of the samples weakly depends on the features of metal and is close to V_Σ of the support. The average pore diameter varies in the range of 7.4–8.6 nm.

The XRD study revealed that M/CNTs are the heterophase samples containing phases of the support (the graphitic carbon phase and the phase of metallic nickel and mixed nickel-magnesium oxide) and active component (see Table and Fig. 1). It should be noted that modification of CNTs with metals virtually does not change the position and half-width of the (002) diffraction maximum (at 2θ ≈ 26°) from (00l) planes, which are typical of

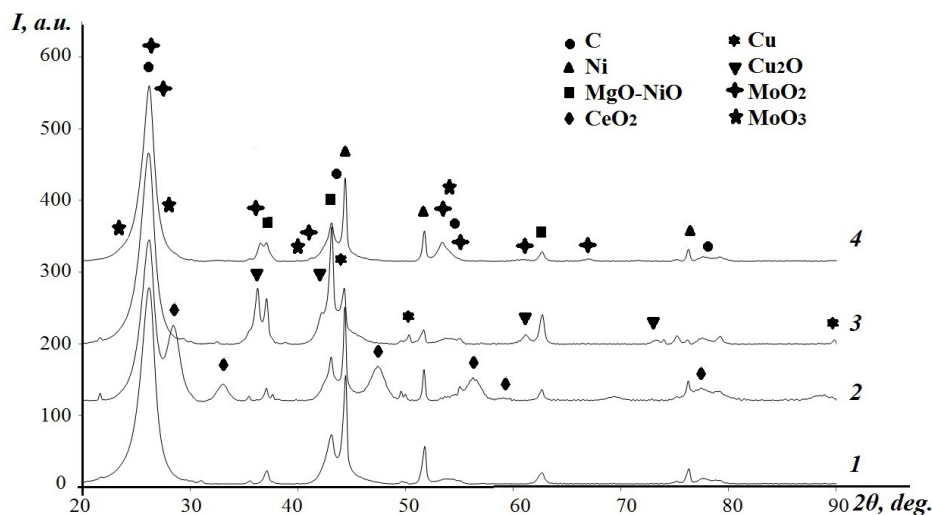


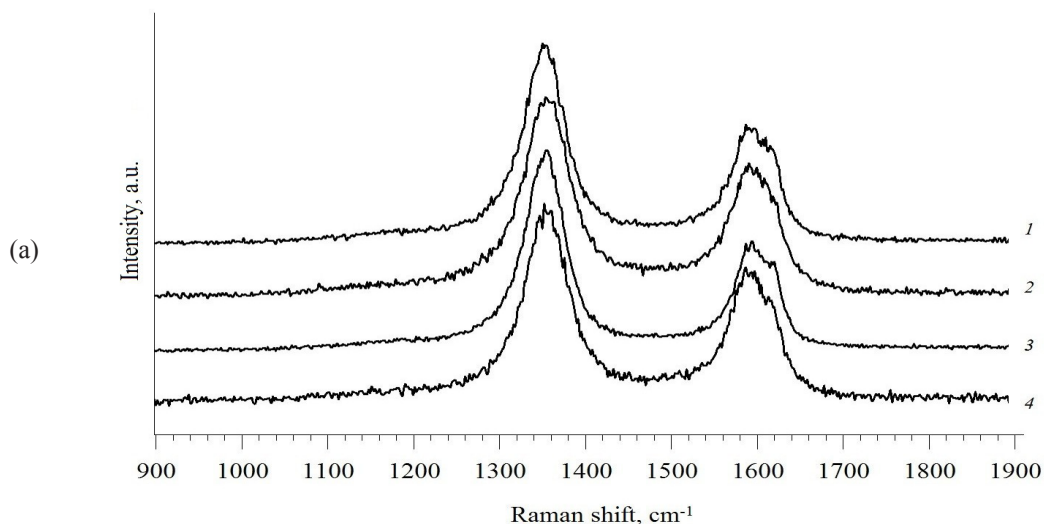
Fig. 1. X-ray diffraction patterns of samples: CNT (1), Ce/CNT (2), Cu/CNT (3) and Mo/CNT (4).

graphitic carbon. The average lattice parameter c is equal to $\sim 6.81 \text{ \AA}$, and the size along the direction perpendicular to graphite layers, $\sim 6 \text{ nm}$. The presence of mixed nickel-magnesium oxide and the metallic nickel phase is caused by the synthesis procedure of CNTs used as the support [29].

Stabilization forms of the active component in the carbon matrix were established. In the case of Ce/CNTs, the active component is represented by highly dispersed cerium dioxide particles. The CSR size of the CeO_2 phase is $\sim 8 \text{ nm}$. For Cu/CNTs, the formation of the copper(I) oxide phase and metallic Cu^0 particles with the CSR size of 20 and 40 nm, respectively, is observed. For Mo/CNT samples, the active component is stabilized as oxides of molybdenum VI and IV, the CSR size of which can hardly be measured because their diffraction maxima cannot be resolved.

The Raman spectroscopy study revealed that

the introduction of active component into the carbon matrix of support and subsequent thermal treatment change the ordering of the carbon framework, which is indicated by changes in the Raman spectra (Fig. 2a) and values of the I_D/I_G ratio (Table) used for estimation of structural defectness. In particular, the decrease in I_D/I_G for M/CNTs ($M = \text{Ce}$ and Mo) in comparison with unmodified CNTs may testify to both a decrease in the fraction of amorphous component of the carbon framework and a decrease in the number of defects [36]. The degree of change in the state of carbon matrix depends on the composition of the active component (Table). One can see that I_D/I_G decreases in the following series of metals: $\text{Cu} > \text{Ce} > \text{Mo}$. It was shown (Fig. 2b) that the active component forms surface oxide structures (CuO , Cu_2O , MoO_x) [37, 38], which is consistent with the XRD data.



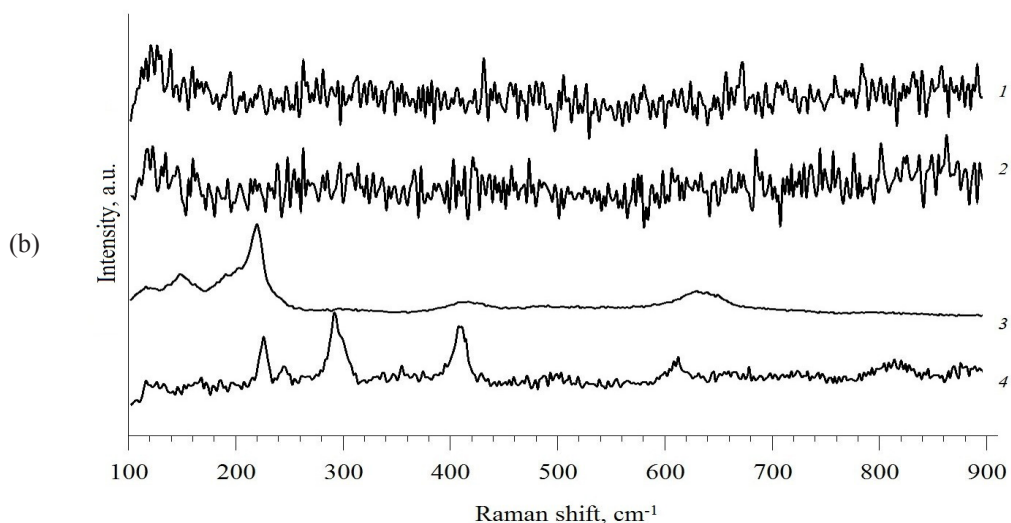


Fig. 2. Raman spectra of samples: CNT (1), Ce/CNT (2), Cu/CNT (3) and Mo/CNT (4) in the spectral range of the Raman shift of $900 \div 1900 \text{ cm}^{-1}$ (a) and $100 \div 900 \text{ cm}^{-1}$ (b).

The SEM study demonstrated that modification of the CNT material with metal salts followed by thermal treatment in an inert atmosphere at $600 \text{ }^\circ\text{C}$ produces virtually no changes in its morphology (Fig. 3). According to EDX mapping, the distribu-

tion of active component depends on the type of metal (Fig. 4). It is seen that the uniformity of metal distribution on the surface of support increases in the series $\text{Cu} < \text{Ce} < \text{Mo}$, which agrees well with the data obtained by structural methods.

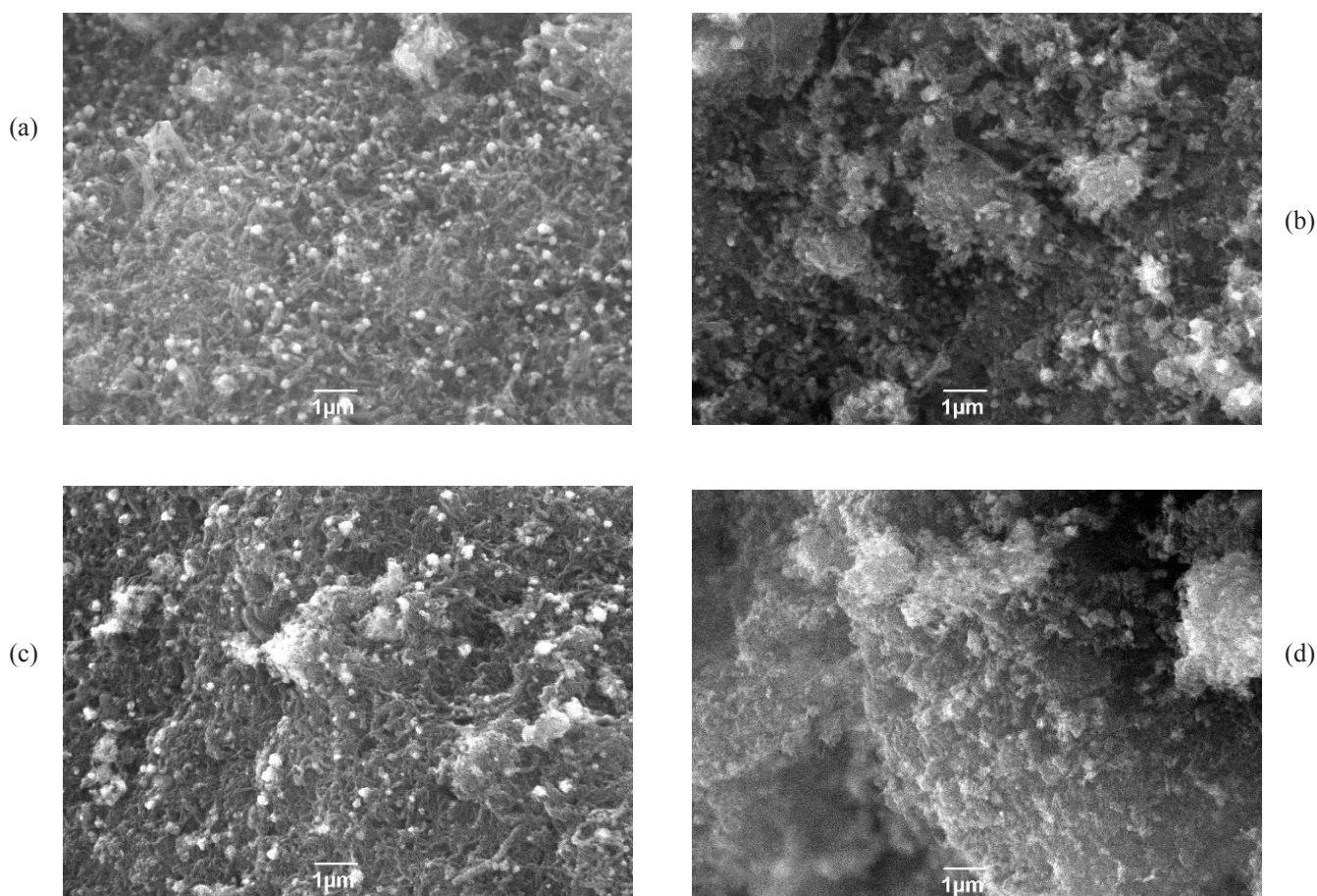


Fig. 3. SEM images of samples: CNT (a), Ce/CNT (b), Cu/CNT (c) and Mo/CNT (d).

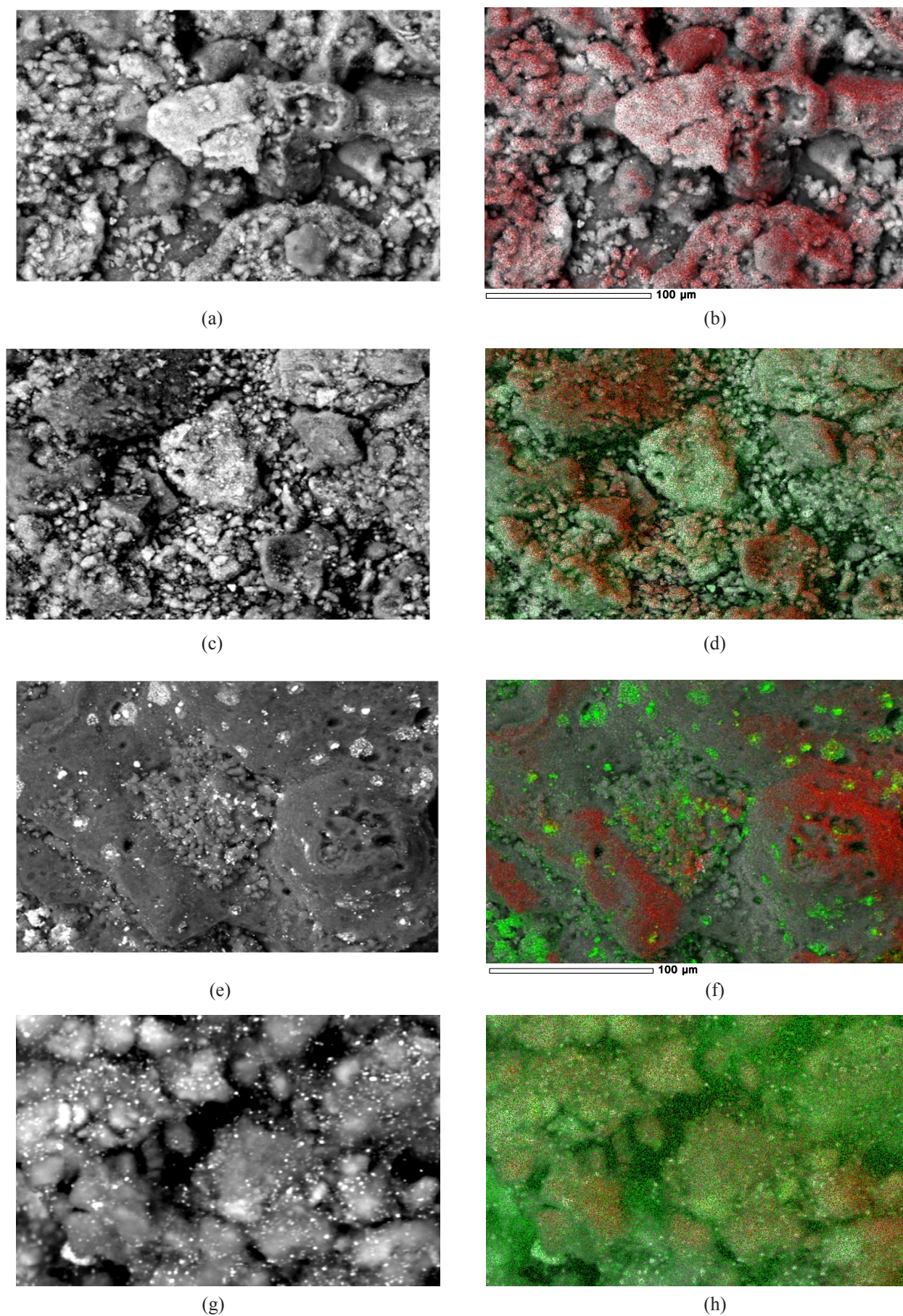


Fig. 4. SEM images of samples: CNT (a, b), Ce/CNT (c, d), Cu/CNT (e, f) and Mo/CNT (g, h), obtained in the registration mode of backscattered electrons (a, c, e, g) and characteristic X-ray radiation O (red), M (green) images (b, d, f, h) with superposition of all signals.

4. Conclusion

A series of metal-carbon materials M/CNTs was synthesized by incipient wetness impregnation with the variation of the type of metal $M = \text{Ce}, \text{Cu}, \text{Mo}$ used for modification of the carbon matrix. Various physicochemical methods were employed to perform a comparative analysis of textural, structural and morphological properties of the samples. It was shown that thermal stability of the samples increases in the series $\text{Ce} < \text{Cu} \approx \text{Mo}$, which is caused by different redox properties of the metals and also by the composition of products of the metal precursor decomposition. It was found that the active component in M/CNTs, $M = \text{Ce}, \text{Cu}, \text{Mo}$, is stabilized on the carbon support surface as CeO_2 , $\text{Cu}_2\text{O}/\text{Cu}$ or $\text{MoO}_3/\text{MoO}_2$ respectively, and its dispersion and deposition uniformity improve in the series $\text{Cu} < \text{Ce} < \text{Mo}$. The synthesized materials are promising for kinetic studies in catalytic ODS of components of diesel fraction from sulfur compound.

Acknowledgments

This study was financially supported by the Russian Science Foundation (Project No. 19-13-00129). This study was accomplished using the research facilities of the Federal Research Center of Coal and Coal Chemistry of SB RAS.

References

- [1]. Ecology and economy: dynamics of air pollution ahead of ratification of the Paris Agreement [Bulletin of current trends in the Russian economy 57 (2019) (in Russian). Electronic resource. Access mode: <https://ac.gov.ru/archive/files/publication/a/23713.pdf>
- [2]. Technical regulation of the Customs Union «On requirements for automobile and aviation gasoline, diesel and marine fuel, jet fuel and fuel oil» TP TC 013/2011 (as amended on December 19, 2019) [Electronic resource]. Access mode: <http://docs.cntd.ru/document/902307833>
- [3]. A. Stanislaus, A. Marafi, M.S. Rana, *Catal. Today* 153 (2010) 1–68. DOI: 10.1016/j.cattod.2010.05.011
- [4]. J.N.D. de Leon., C.R. Kumar, J. Antúnez-García, S. Fuentes-Moyado, *Catalysts* 9 (2019) 87. DOI: 10.3390/catal9010087
- [5]. Z. Ismagilov, S. Yashnik, M. Kerzhentsev, V. Parmon, A. Bourane, F.M. Al-Shahrani, A.A. Hajji, O.R. Koseoglu, *Catal. Rev.* 53 (2011) 199–255. DOI: 10.1080/01614940.2011.596426
- [6]. S.A. Yashnik, A.V. Salnikov, M.A. Kerzhentsev, A.A. Saraev, V.V. Kaichev, L.M. Khitsova, Z.R. Ismagilov, J. Yaming, O.R. Koseoglu, *Kinet. Catal.* 58 (2017) 58–72. DOI: 10.1134/S0023158417010128
- [7]. S.A. Yashnik, A.V. Salnikov, M.A. Kerzhentsev, Z.R. Ismagilov, A. Bourane, O.R. Koseoglu, *Kinet. Catal.* 56 (2015) 466–475. DOI: 10.1134/S0023158415040205
- [8]. S.A. Yashnik, A.V. Salnikov, M.A. Kerzhentsev, Z.R. Ismagilov, J. Yaming, O.R. Koseoglu, *Chemistry for Sustainable Development* 23 (2015) 459–467.
- [9]. Z.R. Ismagilov, M.A. Kerzhentsev, S.A. Yashnik, S.R. Khairulin, A.V. Salnikov, V.N. Parmon, A. Bourane, O.R. Koseoglu, *Eurasian Chem. Tech. J.* 17 (2015) 119–128. DOI: 10.18321/ectj202
- [10]. Patent US 8906227B2. Mild hydrodesulfurization integrating gas phase catalytic oxidation to produce fuels having an ultra-low level of organosulfur compounds. A. Bourane, O.R. Koseoglu, Z.R. Ismagilov, S.A. Yashnik, M.A. Kerzhentsev, V.N. Parmon.
- [11]. Patent US 8920635B2. Targeted desulfurization process and apparatus integrating gas phase oxidative desulfurization and hydrodesulfurization to produce diesel fuel having an ultra-low level of organosulfur compounds. A. Bourane, O.R. Koseoglu, Z.R. Ismagilov, S.A. Yashnik, M.A. Kerzhentsev, V.N. Parmon.
- [12]. US Patent application US 2013/0026072A1. Catalytic compositions useful in removal of sulfur compounds from gaseous hydrocarbons, processes for making these and uses thereof. A. Bourane, O.R. Koseoglu, Z.R. Ismagilov, S.A. Yashnik, M.A. Kerzhentsev, V.N. Parmon.
- [13]. US Patent application US 2016/14/987141. Methods for gas phase oxidative desulphurization of hydrocarbons using CuZnAl catalysts promoted with group VIB metal oxides. Koseoglu, Yaming Jin, Z.R. Ismagilov, S.A. Yashnik, A.V. Salnikov, M.A. Kerzhentsev, V.N. Parmon.
- [14]. International Application WO2013116338 A1. Mild hydrodesulfurization integrating gas phase catalytic oxidation to produce fuels having an ultra-low level of organosulfur compounds. A. Bourane, O.R. Koseoglu, Z.R. Ismagilov, S.A. Yashnik, M.A. Kerzhentsev, V.N. Parmon.
- [15]. M.N. Hossain, H.C. Park, H.S. Choi, *Catalysts* 9 (2019) 229. DOI: 10.3390/catal9030229
- [16]. W.A.W.A. Bakar, R. Ali, A.A.A. Kadir, W.N.A.W. Mokhtar, *Fuel Process. Technol.* 101 (2012) 78–84. DOI: 10.1016/j.fuproc.2012.04.004

- [17]. T. Guo, W. Jiang, Y. Ruana, L. Dong, H. Liu, H. Li, W. Zhu, H. Li, *Colloid. Surface. A* 537 (2018) 243–249. DOI: [10.1016/j.colsurfa.2017.10.016](https://doi.org/10.1016/j.colsurfa.2017.10.016)
- [18]. K.-G. Haw, W.A.W.A. Bakar, R. Ali, J.-F. Chong, A.A.A. Kadir, *Fuel Process. Technol.* 91 (2010) 1105–1112. DOI: [10.1016/j.fuproc.2010.03.021](https://doi.org/10.1016/j.fuproc.2010.03.021)
- [19]. N.M. Meman, B. Zarenezhad, A. Rashidi, Z. Hajjar, E. Esmaeili, *J. Ind. Eng. Chem.* 22 (2015) 179–184. DOI: [10.1016/j.jiec.2014.07.008](https://doi.org/10.1016/j.jiec.2014.07.008)
- [20]. B. Zapata, F. Pedraza, M.A. Valenzuela, *Catal. Today* 106 (2005) 219–221. DOI: [10.1016/j.cattod.2005.07.134](https://doi.org/10.1016/j.cattod.2005.07.134)
- [21]. L.C. Caero, E. Hernandez, F. Pedraza, F. Murrieta, *Catal. Today* 107–108 (2005) 564–569. DOI: [10.1016/j.cattod.2005.07.017](https://doi.org/10.1016/j.cattod.2005.07.017)
- [22]. F.-L. Yu, C.-Y. Liu, B. Yuan, C.-X. Xie, S.-T. Yu, *Catal. Commun.* 68 (2015) 49–52. DOI: [10.1016/j.catcom.2015.04.029](https://doi.org/10.1016/j.catcom.2015.04.029)
- [23]. J.T. Sampanthar, H. Xiao, H. Dou, T.Y. Nah, X. Rong, W.P. Kwan, *Appl. Catal. B.* 63 (2006) 85–93. DOI: [10.1016/j.apcatb.2005.09.007](https://doi.org/10.1016/j.apcatb.2005.09.007)
- [24]. E.V. Rakhmanov, D. Jinyuan, O.A. Fedorova, A.V. Tarakanova, A.V. Anisimov, *Petrol. Chem.* 51 (2011) 216–221. DOI: [10.1134/S0965544111020101](https://doi.org/10.1134/S0965544111020101)
- [25]. A. Corma, P. Concepcio, M. Boronat, M.J. Sabater, J. Navas, M.J. Yacaman, E. Larios, A. Posadas, M.A. Lopez-Quintela, D. Buceta, E. Mendoza, G. Guilera, A. Mayoral, *Nat. Chem.* 5 (2013) 775–781. DOI: [10.1038/nchem.1721](https://doi.org/10.1038/nchem.1721)
- [26]. W. Zhang, H. Zhang, J. Xiao, Z. Zhao, M. Yu, Z. Li, *Green Chem.* 16 (2014) 211–220. DOI: [10.1039/C3GC41106K](https://doi.org/10.1039/C3GC41106K)
- [27]. Q. Gu, G. Wen, Y. Ding, K.-H. Wu, C. Chen, D. Su, *Green Chem.* 19 (2017) 1175–1181. DOI: [10.1039/C6GC02894B](https://doi.org/10.1039/C6GC02894B)
- [28]. CNT series Taunit [Electronic resource]. Access mode: <http://www.nanotc.ru/productions/87-cnm-taunit>
- [29]. Z.R. Ismagilov, S.A. Yashnik, N.V. Shikina, E.V. Matus, O.S. Efimova, A.N. Popova, A.P. Nikitin, *Eurasian Chem. Tech. J.* 21 (2019) 291–302. DOI: [10.18321/ectj886](https://doi.org/10.18321/ectj886)
- [30]. E.V. Matus, L.M. Khitsova, O.S. Efimova, S.A. Yashnik, N.V. Shikina, Z.R. Ismagilov, *Eurasian Chem. Tech. J.* 21 (2019) 303–316. DOI: [10.18321/ectj887](https://doi.org/10.18321/ectj887)
- [31]. C.A. Strydom, C.P.J. van Vuuren, *Journal of Thermal Analysis* 32 (1987) 157–160. DOI: [10.1007/BF01914558](https://doi.org/10.1007/BF01914558)
- [32]. J. Paulik, F. Paulik, M. Arnold, *Journal of Thermal Analysis* 34 (1988) 1455–1466. DOI: [10.1007/BF01914370](https://doi.org/10.1007/BF01914370)
- [33]. M. Nafees, M. Ikram, S. Ali, *Dig. J. Nanomater. Bios.* 10 (2015) 635–641.
- [34]. A. Biedunkiewicz, M. Krawczyk, U. Gabriel-Polrolniczak, P. Figiel, *J. Therm. Anal. Calorim.* 116 (2014) 715–726. DOI: [10.1007/s10973-013-3582-5](https://doi.org/10.1007/s10973-013-3582-5)
- [35]. G. Ciembroniewicz, R. Dziembaj, R. Kalicki, *Journal of Thermal Analysis* 27 (1983) 125–138. DOI: [10.1007/BF01907328](https://doi.org/10.1007/BF01907328)
- [36]. R.A. DiLeo, B.J. Landi, R.P. Raffaele, *J. Appl. Phys.* 101 (2007) 064307. DOI: [10.1063/1.2712152](https://doi.org/10.1063/1.2712152)
- [37]. Deniz Cakir. Enhanced Raman signatures on copper based-materials. Université Montpellier, 2017. English. 179 p.
- [38]. M. Dieterle, G. Mestl, *Phys. Chem. Chem. Phys.* 4 (2002) 822–826. DOI: [10.1039/B107046K](https://doi.org/10.1039/B107046K)